Journal of Science Research

Computational studies of the corrosion inhibition potentials of some derivatives of 1H-Imidazo [4, 5-F] [1, 10] phenanthroline

Obi-Egbedi, N. O. [1] and **Ojo, N. D.**[2]*
Department of Chemistry, Faculty of Science, University of Ibadan, Ibadan, Nigeria
Correponding author: dammynath@yahoo.com

Abstract

Computational simulations of the corrosion inhibition potentials of four imidazophenanthroline derivatives were carried out using Density Functional Theory (DFT) with B3LYP/6-31G* method. It was shown that the predictive corrosion inhibition potentials increase in the order 2-methyl-1H-imidazo[4,5-f][1,10]phenanthroline (MIP) < 3-(1H-imidazo [4, 5-f][1, 10] phenanthrolin-2-yl) phenol (IPP) <2-(2-methoxyphenyl)-1H-imidazo [4, 5-f] [1, 10] phenanthroline (MPIP) < 4-methoxy-2-(3H-phenanthro [9, 10-d] imidazol-2-yl) phenol (MPP). The anticorrosion potentials were predicted using the quantum chemical parameters like energy gap (ΔE), energy of highest occupied molecular orbital (E_{HOMO}), energy of lowest unoccupied molecular orbital (E_{LUMO}), ionization potential (I), electron affinity (A), polarizability (α), global hardness (η), global softness (ó), electronegativity (*x*) and polar surface area (PSA). Corrosion inhibition potentials increase with increasing E_{HOMO}, polarizability, global softness and polar surface area (PSA), and decreasing energy gap (ΔE), E_{LUMO} and global hardness. Also, the sites of likely electrophilic attack were located on nitrogen and oxygen atoms as shown by high negative Mulliken charges of these atoms. This implied that the metal surface atoms could be bonded to these inhibitors through nitrogen and oxygen atoms. From the results, 4-methoxy-2-(3H-phenanthro [9, 10-d] imidazol-2-yl) phenol (MPP) showed the highest E_{HOMO}, polarizability, PSA, and the lowest ÄE, E_{LUMO}, hence the greatest potential of inhibiting corrosion of metals in aqueous solutions.

Keywords: Imidazophenanthroline; corrosion; inhibition potentials; computational studies; Density Functional Theory.

Introduction

Corrosion is the deterioration of the properties of a material as a result of its interaction with its environment [1]. This process is electrochemical and more often than not spontaneous due to the intrinsic tendency of materials to return to their natural states. In the presence of corroding environment that is commonly used by construction companies, materials composing of aluminium and mild steel tend to get oxidised, thereby losing their characteristic malleability and ductility. This mechanical failure has always led to the collapse of important constructions like bridges, oil pipes, refineries, buildings among others [2]. Therefore, it is crucial to forestall and prevent this destructive process.

Various corrosion prevention methods have been widely used without compromising environmental health while ensuring cost effectiveness. The use of organic heterocyclic compounds and substances extracted from different plant parts as corrosion inhibitors has been recently adopted [2-14]. Molecules with heteroatoms like nitrogen, sulphur and oxygen have been reported to possess corrosion inhibition properties [6,15]. When added to corroding environment in small quantities, these molecules have the tendency of being adsorbed on metal surfaces, thereby preventing the cathodic or anodic process and, hence, retarding the rate of corrosion [16]. One of such molecules is imidazo [4, 5F] [1, 10] phenanthroline derivatives [7, 17, 18].

Researches have been conducted and reported on the synthesis and complexation of imidazo [4, 5-F] [1, 10] phenanthroline derivatives [19, 20]. Further researches have been conducted on the corrosion inhibition properties of 2-(6-methylpyridin-2-yl) oxazolo [5, 4-F] [1, 10] phenanthroline. It was reported that

the molecules showed excellent corrosion inhibition properties towards mild steel in 0.5M H_2S0_4 and the active sites of adsorption were the nitrogen and oxygen atoms of the molecule [7]. In addition, anticorrosion potentials of 2-mesityl-1H-imidazo [4, 5-F] [1, 10] phenanthroline have been reported using experimental and computational methods, and both methods showed a good agreement [18]. These anticorrosion potentials of imidazo [4, 5-F] [1, 10] phenanthroline derivatives are as a result of their molecular properties. Also, the presence of nonbonding and π-electron active sites makes the inhibitors susceptible to electrophilic attack [18, 20].

Computational methods have been recently employed to model the molecular properties of organic, inorganic and condensed matter [5-8, 17, 21-26]. Researchers have correlated these molecular properties to the corrosion inhibition properties of such molecules [9, 23, 27, 28]. One of such computational methods is Density Functional Theory (DFT) that models the ground state electronic properties of a system as a function of its electron density. One of the advantages of these computational methods over experimental methods is that data collected and analysed experimentally are prone to statistical error, which is absent in computational techniques [23].

Therefore, this work aims at the computational studies of the corrosion inhibition potentials of four derivatives of imidazo [4, 5-F] [1, 10] phenanthroline (Figures 1-4) using DFT method to simulate the molecular and electronic properties of these compounds.

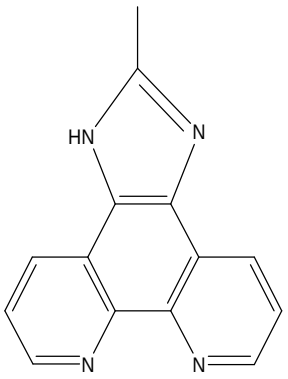

Figure 1. MIP: 2-methyl-1H-midazol; 4, 5-f] [1, 10] phenanthroline.

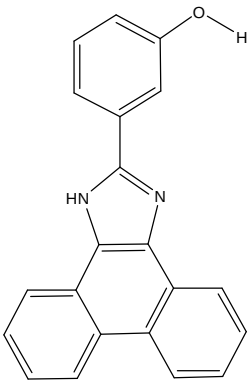

Figure 2. IPP: 3-(1H-imidazol [4, 5-f] [1, 10] phenanthrolin-2-yl0 phenol.

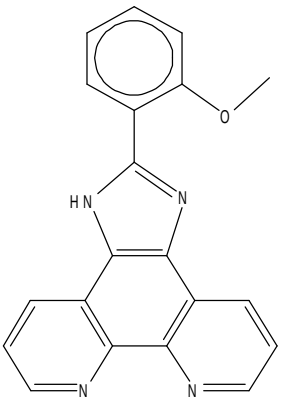

Figure 3. MPIP: 2-2(2-methoxy phenly)-1H-imidazol [4, 5-f] [1, 10] phenanthroline.

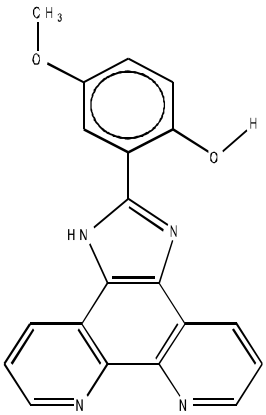

Figure 4. MPP: 4-methoxy-2-(3H-phenanthro [9, 10-d] imidazol-2-yl) phenol.

Computational details

Computational simulation of the molecular properties of imidazo [4, 5-F] [1, 10] phenanthroline derivatives were carried out using Density Functional Theory (DFT) in Spartan 10 programme package [29]. Full geometry optimization was carried out on the equilibrium geometry of the four molecules athybrid Becke-3-Lee-Yang-Parr exchange-correlation functional method with double zeta 6-31G(d) basis set[B3LYP/6-31G(d)] level of theory. Figures 8, 9, 13 and 17 show the B3LYP optimized structures of MIP, IPP, MPIP and MPP respectively. DFT has proven to be a powerful method of calculating the ground state molecular properties of a molecule with a good accuracy. Also, this method is adopted to simulate the molecular properties, reactivity and selectivity of an *N*-electron system using such quantum chemical parameters as energy gap (ΔE), global hardness (η), global softness (σ), ionization energy (I) and electron affinity (A).

Results and discussion

It has been reported that the corrosion inhibition potential of a molecule is related to its electronic properties [15] which can be deduced from its quantum chemical parameters such as energy gap ($\Delta E = E_{LUMO} - E_{HOMO}$), global hardness and global softness [7, 17, 30]. These parameters are reported in Table 1.

The energy gap is a vital index of stability of a system. The wider the energy gap, the more stable a molecule is, hence, the less its reactivity [23]. It is the difference between the energies of highest occupied molecular orbital (E_{HOMO}) and the lowest unoccupied molecular orbitals (E_{LUMO}) [18].

The ability of an inhibitor to donate electrons into the low-lying vacant orbitals of a metal is a function of its ionization potential (I) which is related to the energy of highest occupied molecular orbital, E_{HOMO}, by the expression:

$$I = -E_{HOMO} \quad \ldots . (1)$$

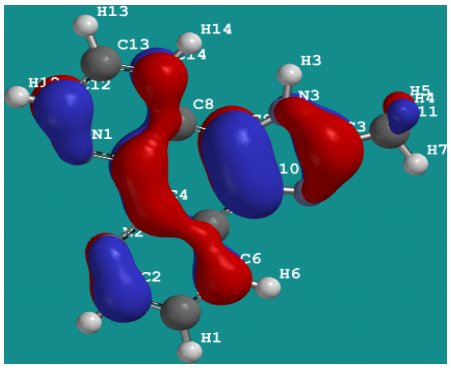

Figure 5. HOMO plot of MIP.

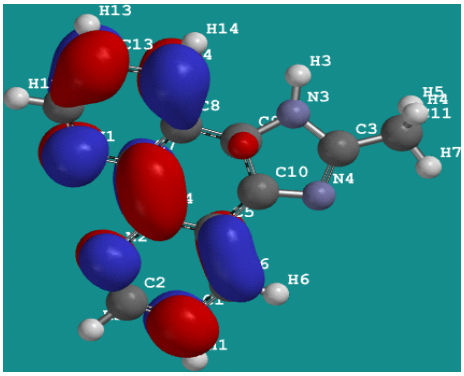

Figure 6. LUMO plot of MIP.

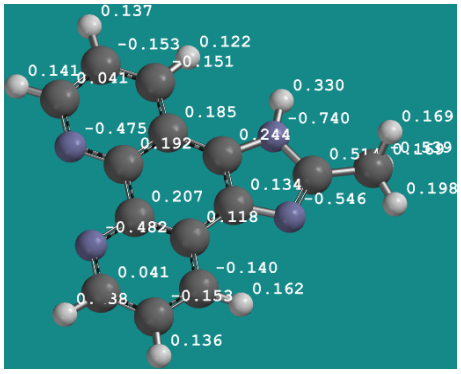

Figure 7. Mulliken charge population analysis of MIP.

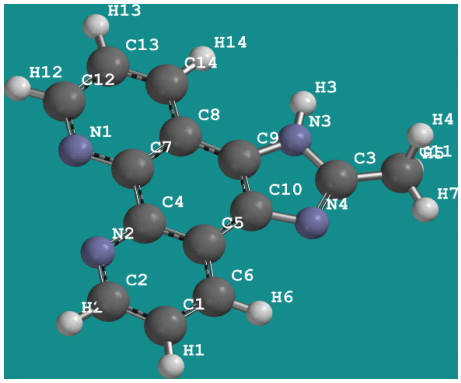

Figure 8. B3LYP optimized structure of MIP.

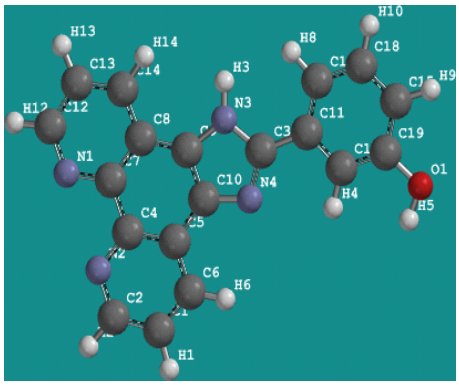

Figure 9. B3LYP Optimized Structure of IPP.

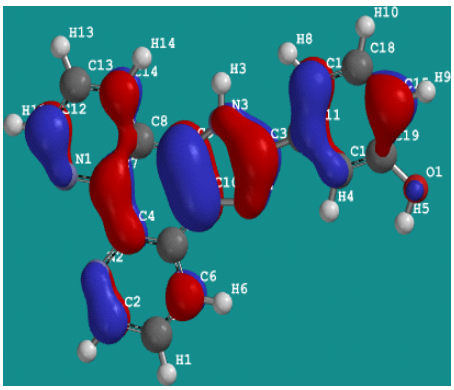

Figure 10. HOMO plot of IPP.

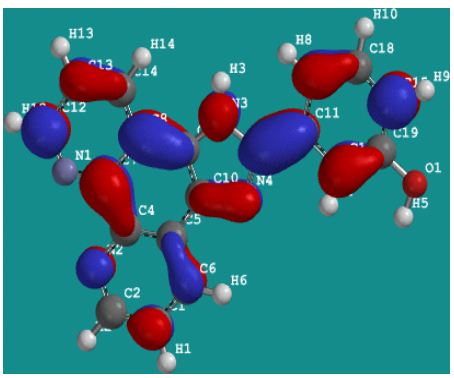

Figure 11. LUMO Plot of IPP.

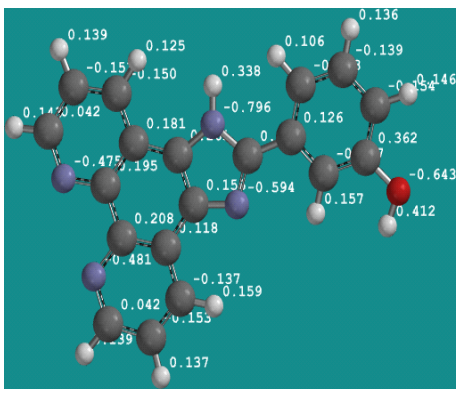

Figure 12. Mulliken charge population analysis of IPP.

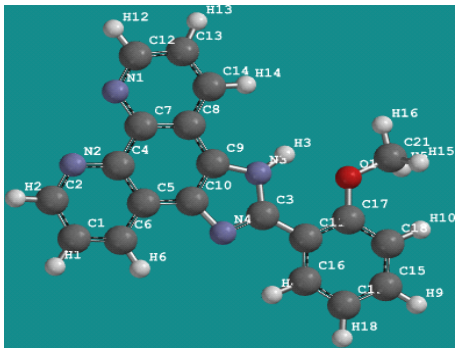

Figure 13. B3LYP Optimized Structure of MPIP.

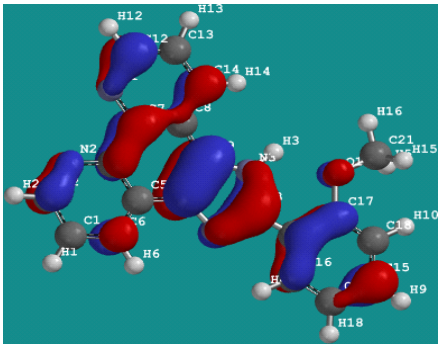

Figure 14. HOMO plot of MPIP.

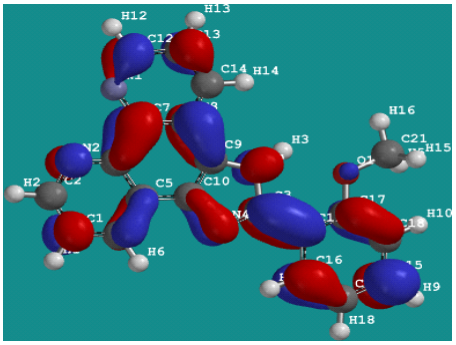

Figure 15. LUMO Plot of IPP.

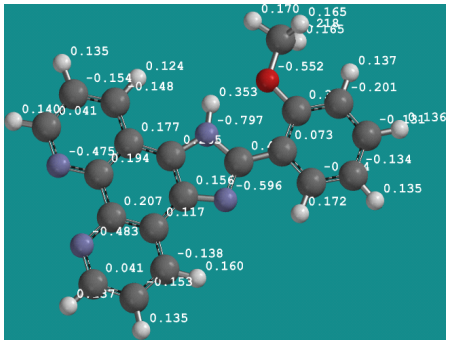

Figure 16. Mulliken charge population analysis of IPP.

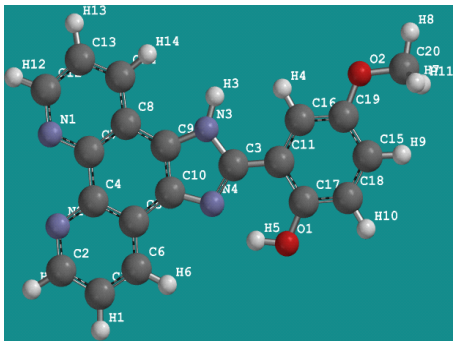

Figure 17. B3LYP Optimized Structure of MPP.

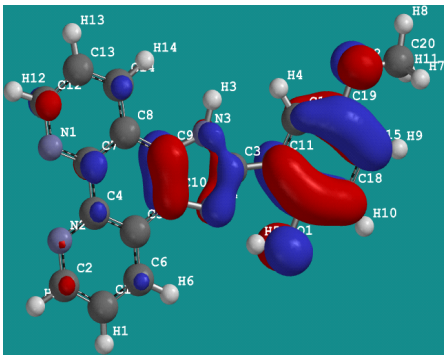

Figure 18. HOMO plot of MPP

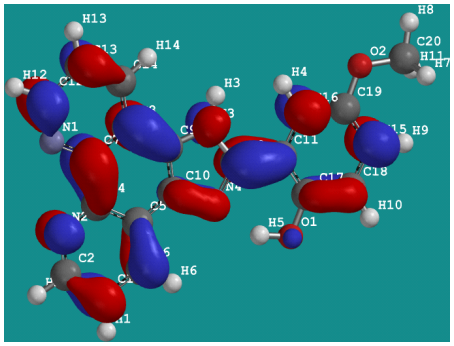

Figure 19. LUMO plot of MPP.

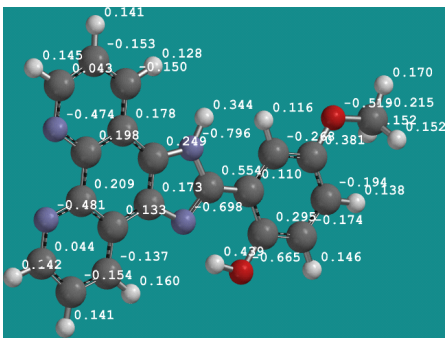

Figure 20. Mulliken charge population analysis of MPP.

Also, the electron affinity (A) of an inhibitor is related to the energy of lowest unoccupied molecular orbital, $E_{LUMO,}$ and it indicates the tendency of the inhibitor to accept electrons.

$$A = -E_{LUMO} \quad \ldots (2)$$

As the energy gap (ΔE) of inhibitors decreases, there is a corresponding increase in their reactivity, hence, an increase in the predictive corrosion inhibition potential. This band gap is related to *I* and *A* by the expression:

$$\Delta E = I - A \quad \ldots . (3)$$

Another parameter related to I and A is the global hardness (η) [31]. This parameter is used to predict the reactivity of a molecule and it is the reluctance of a system to release electrons. It originates from Lewis theory and the theory of Hard and Soft Acid and Base (HSAB). η is defined as the second derivative of electronic energy (E) with respect to number of electrons (N) at constant external potential ($v_{(r)}$):

$$\eta = \left(\frac{\delta^2 E}{\delta N^2} \right) \quad \ldots .(4)$$

$$\eta = \tfrac{1}{2}(I - A) \quad \ldots . (5)$$

This equation can otherwise be written in terms of E_{HOMO} and E_{LUMO} as:

$$\eta = \tfrac{1}{2}(E_{\mathrm{LOMO}} - E_{\mathrm{HOMO}}) \quad \ldots . (6)$$

Global softness (σ) is the half of the reciprocal of global softness and it is another index of chemical reactivity [27]:

$$\sigma = \frac{1}{2\eta} \quad \ldots . (7)$$

Electronegativity, χ, is a descriptor of the direction of electron flow between a metal and an inhibitor until the same chemical potential is attained between the two, and the parameter is used to calculate Δ*N* (number of transferred electrons) [32]. It is related to *I* and *A*, hence E_{HOMO} and E_{LUMO} of a molecule by the expression:

$$\chi = \tfrac{1}{2}(I + A) \quad \ldots . (8)$$

$$\chi = -\tfrac{1}{2}(E_{HOMO} + E_{LUMO}) \quad \ldots . (9)$$

Mulliken atomic charge is an indicator of charge distribution on the atoms of a molecule. The greater the magnitude of the negative charges on atoms, the greater the ease of electron donation by the atom to unoccupied orbitals of a metal [6]. This charge population analysis also gives an indication of the reactivity of the molecule. The Mulliken charge population analysis of MIP, IPP, MPIP and MPP are shown in Figures 7, 12, 16 and 20 respectively. The oxygen and nitrogen atoms show high magnitude of negative charges and are thus the most predictive sites of adsorption by metals [11, 18].

Table 1. Quantum chemical parameters of MIP, IPP, MPIP and MPP using DFT at B3LYP/6-31G(d) level of theory.

Quantum Chemical Parameters	**MIP**	**IPP**	**MPIP**	**MPP**
Energy aq (a.u.)	-758.58	-1025.54	-1064.84	-1140.14
Energy (a.u.)	-758.55	-1025.51	-1064.82	-1140.04
E_{HOMO}	-5.69	-5.60	-5.37	-5.35
E_{LUMO}	-1.25	-1.44	-1.27	-1.49
ΔE (eV)	4.44	4.16	4.10	3.86
Ionisation Potential (I)	5.69	5.60	5.37	5.35
Electron Affinity (A)	1.25	1.44	1.27	1.49
Polarizability (α)	59.31	65.27	66.85	67.44
PSA ($Å^2$)	34.40	52.65	35.75	53.96
Area ($Å^2$)	246.37	315.79	333.76	341.38
Volume ($Å^3$)	234.05	306.67	326.05	342.36
Weight (amu)	234.26	312.33	326.36	342.36
H	2.22	2.08	2.05	1.93
Σ	0.23	0.24	0.24	0.26
X	3.47	3.52	3.32	3.42

Polarizability is the parameter that determines the readiness of the electron cloud of a system to be distorted in a weak applied electric field due to asymmetric molecular charge distribution. It is often observed that polarizability increases with increasing molecular size. Table 1 shows that as the molecular size is increasing in the order MIP<IPP<MPIP<MPP, so also the polarizability increases in the same order. This order provides an indication of the trend of increasing adsorptive properties and corrosion inhibition potentials of the molecules.

The molecular size of a system, as well as the effective surface coverage, is described by such parameters as the polar surface area (PSA), area, molecular volume and weight. Polar Surface Area is the sum over all polar atoms (e.g. N, O, S and P) including attached hydrogen atoms in a given system [33]. All these parameters determine how effectively an inhibitor can be adsorbed on a metal surface and isolate the metal from corroding environment. As the magnitude of these molecular parameters increases, so also the likely anticorrosion potentials of the molecules increase [34-36].

Figures 5, 10, 14 and 18 show the HOMO density distribution indicating that the electron cloud was dispersed over the molecules due to the presence of heteroatoms and π-electrons all over the molecules and show the points susceptible to electrophilic attack. However, Figures 6, 11, 15 and 19 show the LUMO density distributions which are the regions susceptible to nucleophilic attack.

Conclusion

1. MIP, IPP, MPIP and MPP possess corrosion inhibition potentials as can be deduced from their quantum chemical parameters.
2. Corrosion inhibition potential is in the order MIP<IPP<MPIP<MPP.
3. MPP therefore has the least global hardness, smallest energy gap and the greatest global softness, hence the greatest corrosion inhibition potential.

Acknowledgment

The authors acknowledged the effort of Dr. Eseola A.O. in synthesizing these imidazophenanthroline derivatives.

References

[1] Ajanaku, K. O., Aladesuyi, O., Ajanaku, C. O., Adedapo, E. A., Akinsiku, A. A. and Sodiya, F. E. 2015. Adsorption properties of *Azadirachta indicia* extract on corrosion of Aluminium in 1.85 M Hydrochloric acid. *Journal of The International Association of Advanced Technology and Science. 16(04):* 1-11.

[2] Buchweishaija, J. 2009. Plants as a source of green corrosion inhibitors: the case of gum exudates from acacia species.*Tanzanian Journal of Science. 35*: 93-105.

[3] Chitra, S., Parameswari, K., Sivakami, C. and Selvaraj, A. 2010. Sulpha Schiff Bases as Corrosion Inhibitors for Mild Steel in 1M Sulphuric Acid.*Chemical Engineering Research Bulletin. 14:* 1-6.

[4] Essien, K. E., Obot, I. B. and Ebenso, E. E. 2011. 1,2-Diaminoanthraquinone as Corrosion Inhibitor for Mild Steel in Hydrochloric Acid: Weight Loss and Quantum Chemical Study. *International Journal Electrochemical Sci*ence. *6*: 913-930.

[5] Obot, I. B., Ebenso, E. E., Obi-Egbedi, N. O., Afolabi, A. S. and Gasem, Z. M. 2012. Experimental and theoretical investigations of adsorption characteristics of itraconazole as green corrosion inhibitor at a mild steel/hydrochloric acid interface. *Research on Chemical Intermediates. 38*: 1761-1779.

[6] Obot, I. B., Ebenso, E. E., Akpan, I. A., Gasem, Z. M. and Afolabi, A. S. 2012. Thermodynamic and Density Functional Theory investigation of sulphathiazole as green corrosion inhibitor at mild steel / hydrochloric acid interface. *International Journal of Electrochemical Science. 7*: 1978-1996.

[7] Obot, I. B., Ebenso, E. E., Afolabi, A. S. and Oguzie, E. E. 2013. Experimental, quantum chemical calculations, and molecular dynamic simulations insight into the corrosion inhibition properties of 2-(6-methylpyridin-2-yl) oxazolo [5, 4-f] [1, 10] phenanthroline on mild steel. *Research on Chemical Intermediates. 39*: 1927-1948.

[8] Obot, I. B. and Madhankumar, A. 2015. Enhanced corrosion inhibition effect of tannic acid in the presence of gallic acid at mild steel/HCl acid solution interface. *Journal of Industrial and Engineering Chemistry*, *25:*105-111.

[9] Obot, I. B. and Obi-Egbedi, N. O. 2011. Anti-corrosive properties of xanthone on mild steel corrosion in sulphuric acid: Experimental and theoretical investigations. *Current Applied Physics. 11*(3): 382-392. doi:10.1016/j.cap.2010.08.007.

[10] Quraishi, M. A., Ansari, K. R., Yadav, D. K. and Ebenso, E. E. 2012. Corrosion inhibition and adsorption studies of some barbiturates on mild steel/acid interface, *International Journal of Electrochemical Science, 7*: 12301-12315.

[11] Shanmughan, S. K., Kakkassery, J. T., Raphael, V. P. and Kuriakose, N. 2015. Electrochemical and AFM studies on adsorption behaviour of a Polynuclear Schiff Base at carbon steel in HCl medium,*Current Chemistry. Letters, 4*: 1-10.

[12] Singh, A., Ebenso, E. E. and Quraishi, M. A. 2012. Corrosion inhibition of carbon steel in HCl solution by some plant extracts. *International Journal of Corrosion. 2012:* 1-20.

[13] Singh, A. K. and Quraishi, M. A. 2012. Study of some bidentate schiff bases of isatin as corrosion inhibitors for mild steel in hydrochloric acid solution. *International Journal of Electrochemical Science, 7*: 3222-3241.

[14] Upadhyay, R. K. and Mathur, S. P. 2007. Effect of Schiff's bases as corrosion inhibitors on mild steel in sulphuric acid. *E-Journal of Chemistry, 4*(3): 408-414.

[15] Xavier, G.T., Thirumalairaj, B. and Jaganathan, M. 2015. Effect of piperidin-4-ones on the corrosion inhibition of mild steel in 1 N H_2SO_4. *International Journal of Corrosion, 2015:* 1-15.

[16] Porcayo-Calderon, J., Regla, I., Vazquez-Velez, E., Martinez de la Escalera, L.M., Canto, J. and Casales-Diaz, M. 2015. Effect of the unsaturation of the hydrocarbon chain of fatty-amides on the co_2 corrosion of carbon steel using eis and real-time corrosion measurement. *Journal of Spectroscopy, 2015:* 1-13. Retrieved from http://dx.doi.org/10.1155/2015/184140

[17] Junaedi, S., Al-amiery, A. A., Kadihum, A. and Kadhum, A. A. H. 2013. Inhibition effects of a synthesized novel 4-aminoantipyrine derivative on the corrosion of mild steel in hydrochloric acid solution together with quantum chemical studies. *International Journal of Molecular Sciences. 14:* 11915-11928.

[18] Obot, I. B. and Eseola, A. O. 2010. Anticorrosion Potential of 2-Mesityl-1H-imidazo [4, 5-f] [1, 10]-phenanthroline on mild steel in sulfuric acid solution: experimental and theoretical study. *Industrial and Engineering Chemistry Research. 50(4):* 2098-2110.

[19] Eseola, A. O., Li, W., Gao, R., Zhang, M., Hao, X., Liang, T., Obi-Egbedi N.O. and Sun W. 2009. Syntheses, structures and fluorescent properties of 2-(1H-imidazol-2-yl) phenols and their neutral Zn (II) complexes. *Inorganic Chemistry, 48:* 9133-9146.

[20] Zheng, Z., Zhi-Peng, Y., Hong-Ping, Z., Jia-Xiang, Y., Yan, F., Lin, K., Jie-Ying, W. and Yu-Peng, T. 2012. A new imidazophenanthroline derivative and its Hg (II) complex structures, photophysical properties, and DFT calculations. *Journal of Coordination Chemistry. 65(22):* 3972-3982.

[21] Döner, A., Solmaz, R., Özcan, M. and Kardas, G. 2011. Experimental and theoretical studies of thiazoles as corrosion inhibitors for mild steel in sulphuric acid solution. *Corrosion Science, 53*: 2902-2913.

[22] Obi-Egbedi, N. O., Essien, K. E. and Obot, I. B. 2011. Computational simulation and corrosion inhibitive potential of alloxazine for mild steel in 1M HCl. *Journal of Computational Methods of Molecular Design, 1*(1): 26-43.

[23] Gece, G. 2008. The use of quantum chemical methods in corrosion inhibitor studies. *Corrosion Science, 50(11):* 2981-2992.

[24] Kabanda, M. M., Obot, I. B. and Ebenso, E. E. 2013. Computational study of some amino acid derivatives as potential corrosion inhibitors for different metal surfaces and in different media. *International Journal of Electrochemical Science, 8*: 10839-10850.

[25] Obot, I. B., Umoren, S. A. and Ebenso, E. E. 2011. Computational simulation and statistical analysis on the relationship between corrosion inhibition efficiency and molecular structure of some phenanthroline derivatives on mild steel surface. *International Journal of Electrochemical Sci*ence, *6*: 5649-5675.

[26] El Ashry, E. H., El Nemr A., Essawy, S. A. and Ragab, S. 2006. Corrosion inhibitors part 3^1: Quantum chemical studies on the efficiencies of some aromatic hydrazides and Schiff bases as corrosion inhibitors of steel in acidic medium. *ARKIVOC 2006 (xi):* 205-220.

[27] Obot, I. B., Gasem, Z. M. and Umoren, S. A. 2014a. Molecular level understanding of the mechanism of aloes leaves extract inhibition of low carbon steel corrosion: A DFT approach. *International Journal of Electrochemical Science, 9*: 510-522.

[28] Obot, I. B., Gasem, Z. M. and Umoren, S. A. 2014b. Understanding the mechanism of 2-mercaptobenzimidazole adsorption on Fe (II), Cu (II) and Al (III) Surfaces: DFT and molecular dynamics simulations approaches. *International Journal of Electrochemical Science*, *9*: 2367-2378.

[29] Spartan 10 Wavefunction, Inc. 2010. Irvine, CA: Y. Shao, L.F. Molnar, Y. Jung, J. Kussmann, C. Ochsenfeld, S.T. Brown, A.T.B. Gilbert, L.V. Slipehenko, S.V. Levehenko, D.P. O'Neill, R.A. DiStasio Jr., R.C. Lochan, T.Wang, G.J.O. Beran, N.A. Besley, J.M. Herbert, C.Y. Lin, T. Van Voorhis, S.H. Chien, A. Sodt, R.P. Steele, V.A. Rassolov, P.E. Maslen, P.P. Korambath, R.D. Adamson, B. Austin, J. Baker, E.F.C. Byrd, H. Dachsel, R.J. Doerksen, A. Dreuw, B.D. Dunietz, A. D. Dutoi, T.R. Furlani, S.R. Gwaltney, A. Heyden, S. Hirata, C.P. Hsu, G. Kedziora, R. Z. Khalliulin, P.Klunzinger, A. M. Lee, M.S. Lee, W.Z. Liang, I. Lotan, N. Nair, B. Peters, E.I. Proynov, P. A. Pieniazek, Y. M. Rhee, J. Ritchie, E. Rosta, C.D. Sherrill, A. C. Simmonett, J. E. Subotnik, H. L. Woodcock III, W.Zhang, A. T. Bell, A. K. Chakraborty, D.M. Chipman, F.J. Keil, A. Warshel, W.J. Hehre, H.F. Schaefer, J. Kong, A.I. Krylov, P.M.W. Gill and M. Head-Gordon. *Phys. Chem. Chem. Phys. 8:* 3172.

[30] Arslan, T., Kandemirli, F., Ebenso, E. E., Love, I.and Alemu, H. 2009. Quantum chemical studies on the corrosion inhibition of some sulphonamides on mild steel in acidic medium. *Corrosion Science*, *51(1):* 35-47.

[31] Sun, F. and Jin, R. 2013. DFT and TD-DFT study on the optical and electronic properties of derivatives of 1,4-bis (2-substituted-1,3,4-oxadiazole) benzene. *Arabian Journal of Chemistry*, 2-7. doi:10.1016/j.arabjc.2013.11.037.

[32] Scendo, M. and Trela, J. 2013. Corrosion inhibition of carbon steel in acid chloride solution by Schiff base of N-(2-chlorobenzylidene)-4-acetylaniline. *International Journal of Electrochemical Science, 8*: 8329-8347.

[33] Peter E., Bernhard R. and Paul S. 2000. Fast calculation of molecular polar surface area as a sum of fragment-based contributions and its application to the prediction of drug transport properties. Retrieved March 16, 2015, from http://www.peter-ertl.com/reprints/Ertl-JMC-43-3714-2000.pdf

[34] Gece, G. 2011. Drugs: A review of promising novel corrosion inhibitors. *Corrosion Science*, *53(12):* 3873-3898.

[35] https://en.wikipedia.org/wiki/Polar_surface_area. Accessed on February 08, 2016.

[36] Obot, I. B., Macdonald, D. D. and Gasem, Z. M. 2015. Density Functional Theory (DFT) as a powerful tool for designing new organic corrosion inhibitors. Part 1: An overview. *Corrosion Science. 99:*1-30. http://doi.org/10.1016/j.corsci.2015.01.037.